MAGNETIC CHANNEL DESIGN FOR A 250 MeV SUPERCONDUCTING SYNCHROCYCLOTRON*

X.Y. Wu and M.M. Gordon
National Superconducting Cyclotron Laboratory, Michigan State University
East Lansing, MI 48824-1321
U.S.A.

ABSTRACT

A design study has been carried out on a 250 MeV superconducting synchrocyclotron for use in cancer therapy. The extraction system is based on a regenerator followed by a passive magnetic channel, and the properties of the regenerator were described in a previous report. The magnetic channel contains a series of deflecting and focusing elements equipped with projecting wings that are designed to cancel the harmful effects of the fringe fields on the internal beam. Extraction efficiencies for different initial conditions have been calculated using the Z4 Orbit Code which treats all nonlinear effects realistically. In agreement with the conclusions reached at CERN, our results demonstrate the importance of limiting the radial phase space occupied by the beam emerging from the central region.

1. INTRODUCTION

The overall design of our regenerator and magnetic channel was influenced by the extraction system devised for the Harvard synchrocyclotron[1] while the required orbit calculations were modeled on those employed so successfully in upgrading the CERN machine.[2]

Our design process consists of iterating back and forth between magnetic field calculations and orbit computations in order to systematically improve the design parameters and optimize the extraction efficiency. In the magnetic field calculations, we simply assume that the main field is so strong (central field B=57 kG) that the regenerator and channel elements are all uniformly magnetized in the vertical direction, while in the orbit computations, we use our Z4 Orbit Code[3] which provides an accurate evaluation of the important coupling effects between the radial and vertical motion.

*Work supported by the National Science Foundation under Grant No. PHY-86-11210.

Results on the design of the regenerator itself have already been published.[4] The passive magnetic channel consists of a sequence of deflecting and radial focusing elements that bend and focus the beam along its path around the regenerator. These elements are equipped with an elaborate set of "wings" which serve to shelter the internal beam from the extreme vertical overfocusing that would otherwise occur on the last few turns prior to channel entry. Fig.1 shows the nine magnetic channel elements with M1,M2,M5 and M6 being deflecting magnets, while the remainder serve mainly as radial focusing magnets. Fig.2 and Fig.3 show the

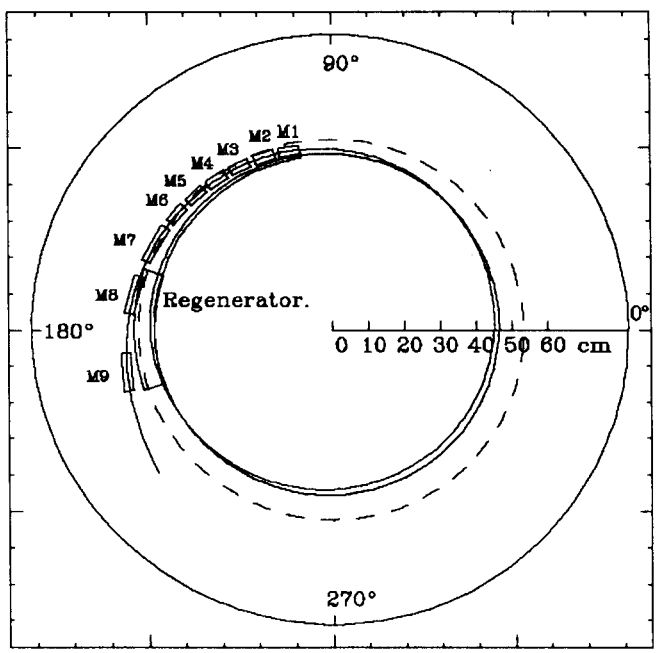

Fig. 1 -- Layout of the Extraction System showing the arrangement of the regenerator and the nine magnetic channel elements. M1,M2,M5, and M6 are deflecting magnets, and M3,M4,M7,M8, and M9 are all focusing magnets. The solid curve shows the last two turns of an extracted orbit, and the broken curve shows the pole boundary.

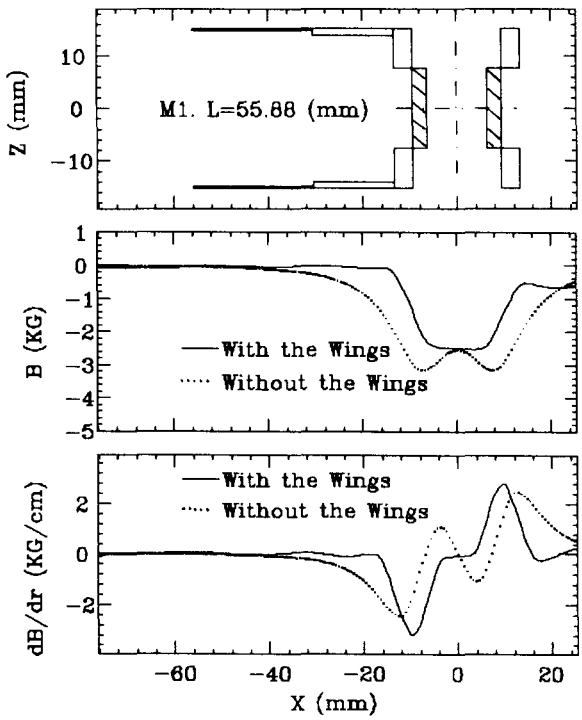

Fig. 2 -- Cross section of the deflecting magnet M1 with its projecting wings. Plots show the resultant field (kG) and field gradient (kG/cm) produced with (solid curve) and without (broken curve) the wings. The effectiveness of the wings is apparent. M2,M5, and M6 are similar.

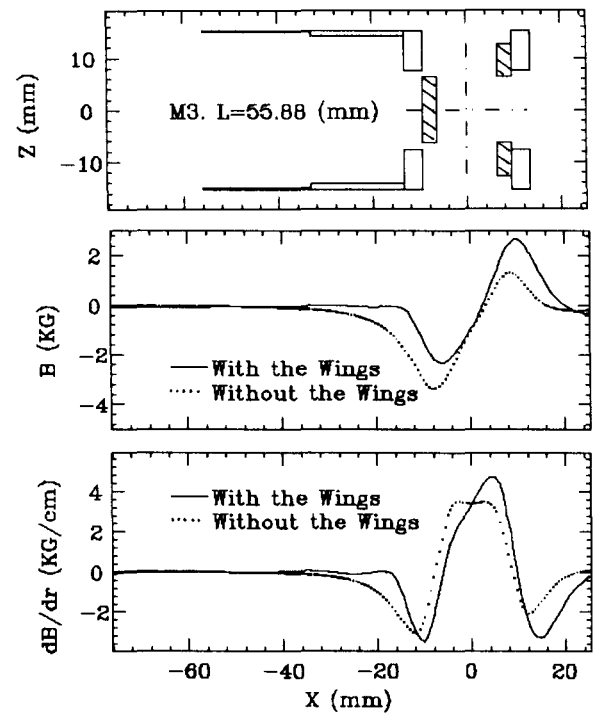

Fig. 3 -- Cross section of the radial focusing magnet M3 with its projecting wings. Plots of resultant field and field gradient are analagous to those in Fig. 2. M4 and M7 are similar in structure, but M8 and M9 do not require wings.

geometries and magnetic properties of two typical elements. The magnetic channel starts at θ=100° with its center at r=50.1 cm. The channel entrance aperture is 12.7 mm and the septum thickness is 3.2 mm.

2. RADIAL MOTION

Fig. 4 shows the four static phase plots at θ=180° and E=254.5 MeV that were used as initial conditions for the accelerated orbits. These plots correspond to radial amplitudes of 1.27, 2.54, 3.81 and 5.08 mm. The approximate stability boundary is also shown. (This boundary shrinks to zero at E=255.7 MeV where $\nu_r = 1$.) Using a constant energy-gain per turn of 10 KeV, the orbits are traced until they are either

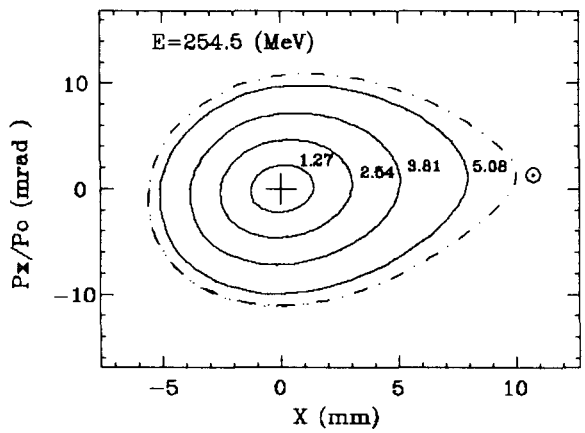

Fig. 4 -- Radial phase plots at E=254.5 MeV and θ=180° showing four invariant curves for radial amplitudes of 1.27, 2.54, 3.81 and 5.08 mm. Between 60 and 74 points on these curves were used as initial conditions for the accelerated orbits. The dot-dash curve shows an approximate stability boundary at this energy.

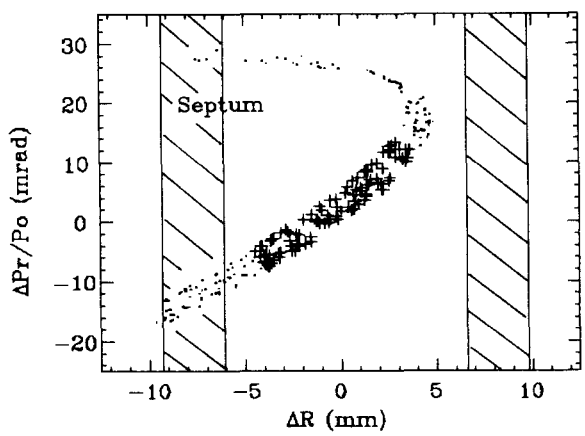

Fig. 5 -- Radial phase plot at the entrance of the magnetic channel (θ=100°) showing resultant distribution for median plane orbits with initial conditions given in Fig. 4. Points labeled with "+" signs indicate those orbits that successfully traverse the magnetic channel. (p_o is the momentum corresponding to E_o=255.0 MeV.)

successfully extracted or lost through hitting an obstacle.

The resulting phase space distribution at the entrance of the magnetic channel is shown in Fig. 5 for the four different radial amplitudes. Plotted here are the differences between the (r,p_r) of the orbits and the (r_o,p_{ro}) of the central ray; also shown are the position and size of the septum. Orbits entering the channel with too small or too large values of p_r hit the inner or outer wall, respectively. About 42% of the orbits are successfully extracted.

3. COMBINED RADIAL AND VERTICAL MOTION

The computations were carried out using the Z[4] Orbit Code which is based on exact equations of motion and magnetic field components that are correct to fourth order in z.[3] The results therefore provide a more realistic evaluation of the effects of the vertical motion. For each of the (r,p_r) values used above at 254.5 MeV, we used eight initial (z,p_z) points uniformly spread around an eigenellipse having a given maximum height Δz_o = 2.54 or 5.08 mm. Fig. 6 shows the initial (z,p_z) conditions used in these computations.

As shown in the work at CERN,[5] orbits with large radial amplitudes produce unacceptable growth in the vertical oscillations due to the $\nu_r = 2\nu_z$ coupling resonance. Our present studies show that the reverse can also be true and that in some cases, the radial and vertical oscillations grow simultaneously to very large amplitudes. Since ν_r = 1 and ν_z = 0.5 in these cases, we attribute this phenomenon to the $\nu_r+2\nu_z=2$ coupling resonance.

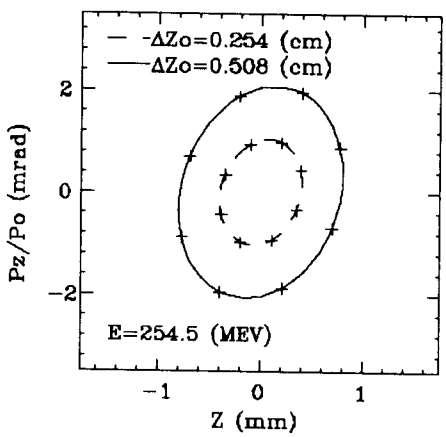

Fig. 6 -- Initial (z,p_z) values at E=254.5 MeV and θ=180° used for accelerated orbits in conjunction with the (r,p_r) values given in Fig. 4. The two eigenellipses shown here have their maximum height Δz_o = 2.54 and 5.08 mm near θ=0.

For the smallest radial amplitude used in these studies, 1.27 mm, the coupling action remains within acceptable bounds and 51% of the orbits are successfully extracted. For the 2.54 mm radial amplitude case, the extraction efficiency drops to 32% with about 12% of the orbits exceeding a vertical amplitude limit of 15 mm prior to reaching the channel. Fig. 7 shows the resultant vertical phase space distribution for all of these two sets of orbits at the entrance to the channel.

The results are very different for the two largest radial amplitudes, 3.81 and 5.08 mm, where 92% of the orbits fail to reach the channel entrance. That is, the coupling effects described above produce vertical amplitudes that are too large for the given aperture, 30 mm. Thus we find that reasonably good extraction efficiency can be achieved only if the internal beam prior to extraction has a maximum radial amplitude of about 3 mm. This is consistant with the results obtained at CERN[2] where the radial amplitude limit is about 10 mm, since our field is about three times higher than the CERN field and one might expect lengths to scale inversely with the field values.

4. CONCLUSIONS

Assuming now that the internal beam can be controlled so that both the radial and vertical amplitudes do not exceed 3 mm, our results indicate that an extraction efficiency of about 40% can be achieved. A plot of the radial and vertical envelopes for the resultant beam as it traverses the magnetic channel is shown in Fig.8, and these results confirm that the beam remains well focused. The corresponding radial and vertical phase space distributions at the exit of the channel are shown in Fig. 9 with resultant emittances of about 20π mm-mrad radially and 30π mm-mrad vertically.

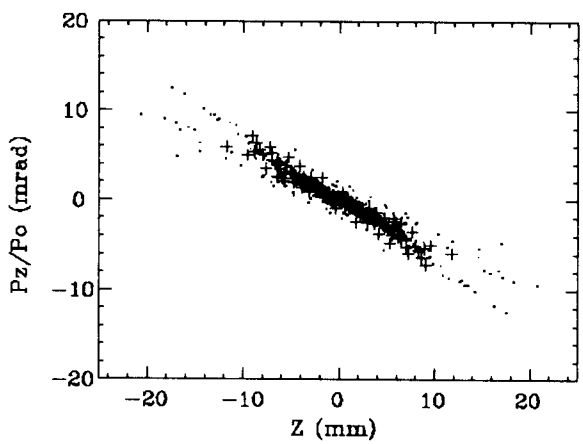

Fig. 7 -- Phase plot at the entrance of the magnetic channel (θ=100°) showing the $(z,p_z/p_o)$ values for all the orbits with initial conditions given in Fig. 6 and Fig. 4 for the two smaller radial amplitudes. Points labeled by "+" signs indicate those orbits that successfully traverse the magnetic channel.

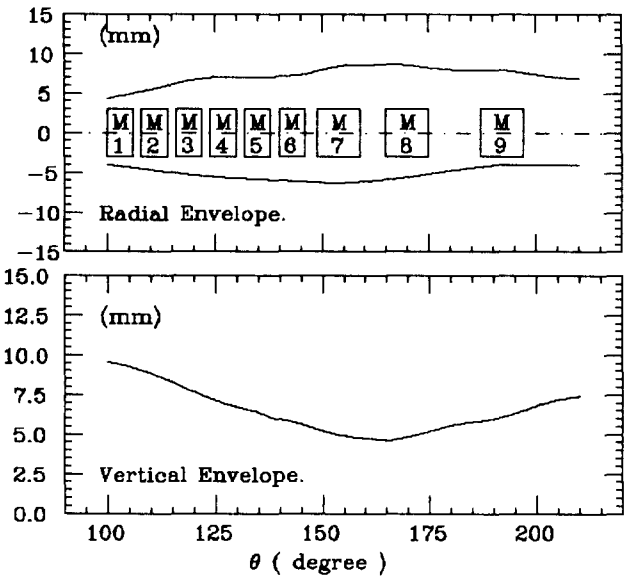

Fig. 8 -- Radial and vertical envelopes for all of the successfully extracted orbits as they traverse the magnetic channel. Plots show $(r-r_o)$ and $|z|$ vs. θ from 100° to 210°. All 145 orbits used here started at 254.5 MeV with initial radial and vertical amplitudes less than 3 mm as shown in Fig. 4 and Fig. 6.

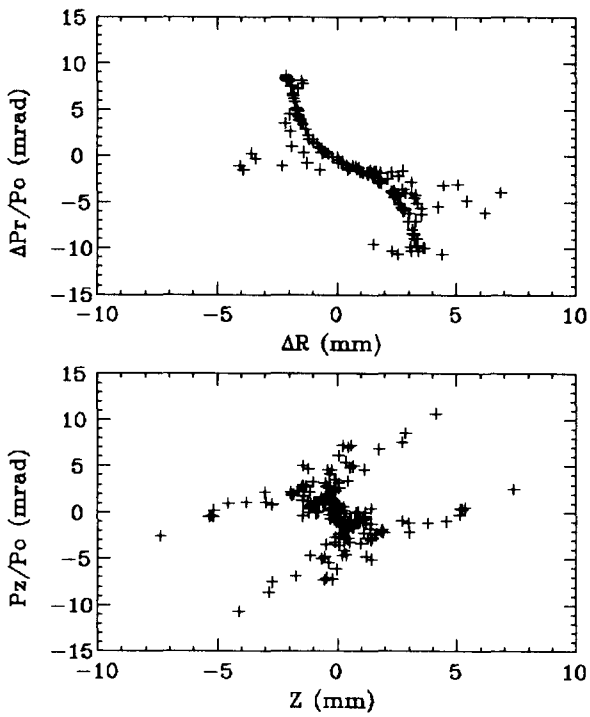

Fig. 9 -- Radial and vertical phase plots at the exit of the magnetic channel (θ=210°) showing the distribution of points for the 145 orbits described in Fig. 8. The estimated final emittances are about 20π mm-mrad radially and 30π mm-mrad vertically.

Finally, the projected energy distribution of the extracted beam is shown in Fig. 10, and indicates an energy spread of about 500 KeV. We should note that this spread depends quite strongly on the vertical amplitude as well as the radial amplitude.

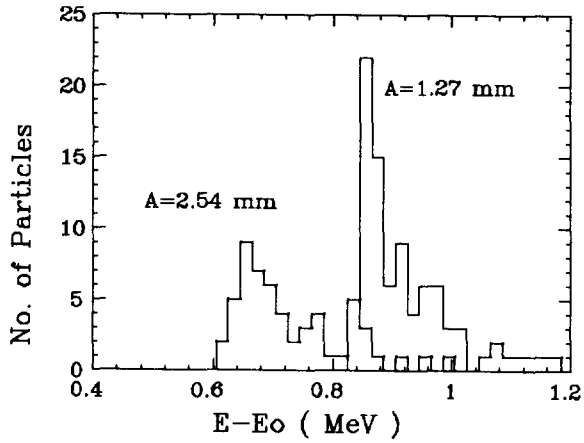

Fig. 10 -- Distribution of final energies for the 145 orbits described in Fig. 8 and Fig. 9. The histograms show the number of extracted orbits vs. $(E-E_o)$ where E_o = 255 MeV, with two separate curves for initial radial amplitudes of 1.27 and 2.54 mm.

REFERENCES

1) G. Calame, et. al., Nucl. Instr. and Meth. I, (1957), pp. 169-182.
2) B. Allardyce, et. al., Proc. 7th Int. Conf. on Cyclotrons and their Applications, (Birkhauser, Basel, 1975), pp. 287-291.
3) M. M. Gordon and V. Taivassalo, Nucl. Instr. and Meth. A247, (1986), pp. 423-430.
4) M. M. Gordon and X. Y. Wu, Proc. of the 1987 Particle Accelerator Conf., (IEEE, New York, 1987), pp. 1255-1257.
5) S. Lindback, Proc. 5th International Cyclotron Conference, (Butterworths, London, 1971), pp. 235-244.